X-ray Absorption Spectroscopic Studies of the Diiron Center in Methane Monooxygenase in the Presence of Substrate and the Coupling Protein of the Enzyme System

Jane G. DeWitt,[†] Amy C. Rosenzweig,[‡] Athanasios Salifoglou,[‡] Britt Hedman,*[,§] Stephen J. Lippard,*[,‡] and Keith O. Hodgson*[,†,§]

Department of Chemistry and Stanford Synchrotron Radiation Laboratory, Stanford University, Stanford, California 94305, and Department of Chemistry, Massachusetts Institute of Technology, Cambridge, Massachusetts 02139

Received August 24, 1994[⊗]

The interaction among the hydroxylase component of methane monooxygenase (MMO) from *Methylococcus capsulatus* (Bath), the coupling protein of the MMO enzyme system (component B), and substrate has been investigated by using Fe K-edge X-ray absorption spectroscopy (XAS). Fe K-edge extended X-ray absorption fine structure (EXAFS) studies of the semimet form of the hydroxylase in the presence of the coupling protein, 1-bromo-1-propene, and both the coupling protein and 1-bromo-1-propene revealed small differences in the appearance of the EXAFS above $k = 8$ Å^{-1} as compared to the noncomplexed hydroxylase. No dramatic change in the Fe coordination was seen in fits to the data. The average first shell Fe−O/N distance for the complexed forms of the semimet hydroxylase ranged between 2.06 and 2.08 Å, which is comparable to the distance found for the noncomplexed form, 2.06−2.09 Å. Although the average first shell coordination was similar for all samples, a difference was seen in the distribution of long vs short distance contributions to the first shell coordination sphere for samples with component B present. This difference was accompanied by a small but consistent decrease in the Fe−Fe distance of the B-complexed hydroxylase samples, from 3.42 to 3.39 Å. When only 1-bromo-1-propene was present, the distance remained unchanged. Similarly, differences were seen in the EXAFS of the reduced forms of the hydroxylase complex above $k = 8.5$ Å^{-1}, but the average Fe coordination as determined by fits to the data was similar to that of the noncomplexed reduced hydroxylase. For the complexed forms of the reduced hydroxylase, an average first shell Fe−O/N distance of 2.11−2.14 Å was found, comparable to the 2.15 Å distance found for the noncomplexed reduced hydroxylase, but a change in the distribution of long vs short distance contributions was again observed when component B was present. High resolution Fe K-edge edge spectra of the B-complexed samples revealed a shoulder on the rising edge of the semimet form of the hydroxylase, suggesting a change in covalency at the Fe site. Furthermore, differences in the edge spectra of the reduced forms of the hydroxylase suggested that the coupling protein and substrate influence the electronic environment of the Fe center. Together, these results show that a subtle change in the Fe environment of the hydroxylase occurs upon complex formation, resulting in a distortion in coordination, a change in the covalency of the Fe center, and/or a change in the ligation of the Fe center. Additionally, comparison of EXAFS results for a brominated model compound to that for 1-bromo-1-propene substrate complexed with hydroxylase provided *no* evidence that the bromine atom of bound substrate is located within about 3.5 Å of an Fe atom. This result makes it unlikely that olefins form a π complex to Fe in the MMO hydroxylase.

Introduction

Soluble methane monooxygenase (MMO) from *Methylococcus capsulatus* (Bath)[1] and *Methylosinus trichosporium* OB3b[2] is a multicomponent enzyme system consisting of a dinuclear non-heme Fe enzyme[3] (hydroxylase, M_r 251K), an Fe_2S_2−FAD electron transport protein[4] (reductase, M_r 38.6K), and a coupling protein (component B, M_r 15.5K) which contains no metals or prosthetic groups.[5] The biological function of MMO is to catalyze the NAD(P)H- and O_2-dependent hydroxylation of methane to methanol in methane-metabolizing bacteria,[6] although a wide variety of organic molecules are oxidized by this enzyme system.[7]

Substrate binding and dioxygen activation occur at the hydroxylase component;[3c,5,8] neither the reductase nor component B is catalytically competent. All three components of the MMO enzyme system are required for efficient oxidation of substrate.[1a,8,9] Kinetic studies on the roles and interaction of the three components of the MMO system from *M. capsulatus* (Bath)[5,9] have suggested the formation of protein complexes

[†] Department of Chemistry, Stanford University.
[‡] Department of Chemistry, Massachusetts Institute of Technology.
[§] Stanford Synchrotron Radiation Laboratory, Stanford University.
[⊗] Abstract published in *Advance ACS Abstracts,* April 1, 1995.

(1) (a) Colby, J.; Dalton, H. *Biochem. J.* **1978**, *171*, 461−468. (b) Colby, J.; Dalton, H. *Biochem. J.* **1976**, *157*, 495−497.
(2) Stirling, D. I.; Dalton, H. J. *Eur. J. Biochem.* **1979**, *96*, 205−212.
(3) (a) Woodland, M. P.; Dalton, H. *Anal. Biochem.* **1984**, *139*, 459−462. (b) Woodland, M. P.; Patil, D. S.; Cammack, R.; Dalton, H. *Biochim. Biophys. Acta* **1986**, *873*, 237−242. (c) Woodland, M. P.; Dalton, H. *J. Biol. Chem.* **1984**, *259*, 53−59.
(4) (a) Colby, J.; Dalton, H. *Biochem. J.* **1979**, *177*, 903−908. (b) Lund, J.; Dalton, H. *Eur. J. Biochem.* **1985**, *147*, 291−296.
(5) Green, J.; Dalton, H. *J. Biol. Chem.* **1985**, *260*, 15795−15801.
(6) Anthony, C. *The Biochemistry of the Methylotrophs*; Academic Press: London, 1982.
(7) (a) Colby, J.; Stirling, D. I.; Dalton, H. *Biochem. J.* **1977**, *165*, 395−402. (b) Green, J.; Dalton, H. *J. Biol. Chem.* **1989**, *264*, 17698−17703.
(8) (a) Fox, B. G.; Froland, W. A.; Dege, J. E.; Lipscomb, J. D. *J. Biol. Chem.* **1989**, *264*, 10023−10033. (b) Andersson, K. K.; Froland, W. A.; Lee, S.-K.; Lipscomb, J. D. *New J. Chem.* **1991**, *15*, 411−415. (c) Fox, B. G.; Liu, Y.; Dege, J. E.; Lipscomb, J. D. *J. Biol. Chem.* **1991**, *266*, 540−550.
(9) (a) Lund, J.; Woodland, M. P.; Dalton, H. *Eur. J. Biochem.* **1985**, *147*, 297−305. (b) Green, H.; Dalton, H. *Biochem. J.* **1989**, *259*, 167−172.

0020-1669/95/1334-2505$09.00/0

during the catalytic cycle which have an effect on the oxygenase activity. The effect of component B on electron transfer and oxygenase activity in the MMO system has been studied for both the *M. capsulatus* (Bath)[5,9,10] and the *M. trichosporium* OB3b.[8,11] In the *M. capsulatus* system, component B appears to play a strict regulatory role, preventing reduction of the hydroxylase in the presence of reductase but absence of substrate[10] and the formation of product in the absence of component B.[5,9] In the *M. trichosporium* system, however, the hydroxylase is reduced in the absence of substrate[11] and product is formed in the absence of component B, although the addition of component B greatly increases the specific activity of the hydroxylase.[8]

Various spectroscopic techniques have been used to gain information about the geometric and electronic structure of the diiron active site in the MMO hydroxylase component (**H**) from both *M. capsulatus* (Bath)[4,10,12,13] and *M. trichosporium* OB3b.[8,11,12,14-16] Extended X-ray absorption fine structure (EXAFS) has proved to be very sensitive to the presence or absence of an oxo bridge in the first coordination sphere of dinuclear Fe centers,[17] such as found in the related protein systems hemerythrin (Hr) and ribonucleotide reductase (RR).[18] EXAFS studies[12] have shown that the diferric form of the *M. capsulatus* (Bath) hydroxylase is a non-oxo-bridged diiron center with a first coordination sphere of ~6 N/O atoms at an average distance of 2.04 Å. The semimet form (prepared by photoreduction) has ~6 N/O atoms at 2.08 Å, and the diferrous form has ~5 N/O atoms at 2.15 Å in its first coordination sphere. The Fe-Fe distance for the oxidized and semimet forms of the hydroxylase was determined to be ~3.4 Å (or ~30 Å depending on the model compound used for extraction of empirical backscattering parameters; see p 9231 in ref 12 for detailed discussion). There was no distinct Fe-Fe contribution to the EXAFS of the ferrous hydroxylase.

Recently, the structure of the active site of the hydroxylase of MMO in its diferric form has been determined by X-ray crystallography at 2.2 Å resolution.[19] The Fe atoms are located as a dinuclear site in a 4 helix bundle, coordinated by a total of 4 glutamate residues, 2 histidine residues, and a single molecule of water. Each Fe atom is coordinated by a single histidine residue, while one glutamate residue bridges the Fe atoms in a bidentate mode and the other glutamate residues are coordinated to Fe in a monodentate mode. Additionally, exogenous hydroxide and acetate ligands bridge the two Fe atoms. The Fe atoms are 3.4 Å apart, in very close agreement with the Fe-Fe distance determined previously by EXAFS spectroscopy.[12] The coordination of each Fe atom to a single histidine residue, the presence of a hydroxo bridge, and the presence of more O-donating ligands than N-donating ligands in the active site are consistent with results obtained earlier by EXAFS[12] and ENDOR[13,15,16b] spectroscopies.

These studies have formed the basis for understanding the mechanism of dioxygen activation and substrate oxidation. Studies of the hydroxylase separated from the other required components of the MMO enzyme system provide only one part of the needed information, however, since all three components are required for activity. Perturbations in the EPR spectra of the hydroxylase in the presence of component B and in the presence of small molecules have been documented, suggesting that complexation with the hydroxylase in some way affects the Fe site.[3c,8c,20] The effects of substrate, component B, and the reductase on the redox potentials of the hydroxylase have also been investigated[10,11] and reveal that significant changes in the electron affinity of the hydroxylase core occur as a function of the presence of the other components. The changes in the redox potentials and the EPR spectra of the complexed forms of the hydroxylase imply an alteration in the electronic structure of the Fe site which could be caused by alterations in the ligation of the diiron site or by conformational changes of the protein near or at the Fe center which affect the electronic properties of the diiron core. EXAFS would be sensitive to any structural changes which occur as a result of the complex formation, and electronic perturbations would have an effect on the edge structure of the hydroxylase complexes.

In the present investigation, Fe K-edge EXAFS and high-resolution edge data on *M. capsulatus* (Bath) hydroxylase samples in the semimet (photoreduced from diferric) and diferrous forms in the presence of component B, a mixture of *cis*- and *trans*-1-bromo-1-propene (hereafter referred to as bromopropene), and both component B and bromopropene have been collected. The goal was to determine what effect, if any, these species have on the coordination environment of the Fe atoms. In addition, since olefins are epoxidized by the MMO system, it was of interest to determine whether bromopropene might coordinate directly to an Fe atom in the catalytic center. Results show that, for the conditions used in this study, no dramatic change in the coordination of the Fe atoms occurs upon formation of the various complexes. Evidence for a subtle change in the coordination environment and in the covalency of the diiron center in the presence of component B and bromopropene is directly and reproducibly seen (*via* multiple samples).

Experimental Section

EXAFS Sample Preparation. A summary of the samples investigated is given in Table 1. The soluble hydroxylase of MMO from *M. capsulatus* (Bath) was isolated, purified, and characterized as previously described.[12] Component B was produced from a strain of *Escherichia coli* containing a plasmid with the gene for B from *M. capsulatus* (Bath).[21] For hydroxylase samples with component B present (designated **HB**), component B was added in the stoichiometric molar ratio of 2:1 B:hydroxylase. For hydroxylase samples to which bromopropene was added (designated **HBr** for samples with bromopro-

(10) (a) Liu, K. E.; Lippard, S. J. *J. Biol. Chem.* **1991**, *266*, 12836-12839; 24859. (b) Liu, K. E.; Lippard, S. J. Unpublished results.
(11) Paulsen, K. E.; Liu, Y.; Fox, B. G.; Lipscomb, J. D.; Münck, E.; Stankovich, M. T. *Biochemistry* **1994**, *33*, 713-722.
(12) DeWitt, J. G.; Bentsen, J. G.; Rosenzweig, A. C.; Hedman, B.; Green, J.; Pilkington, S.; Papaefthymiou, G. C.; Dalton, H.; Hodgson, K. O.; Lippard, S. J. *J. Am. Chem. Soc.* **1991**, *113*, 9219-9235.
(13) (a) Bender, C. J.; Rosenzweig, A. C.; Lippard, S. J.; Peisach, J. *J. Biol. Chem.* **1994**, *269*, 15993-15998. (b) DeRose, V. J.; Liu, K. E.; Kurtz, D. M., Jr.; Hoffman, B. M.; Lippard, S. J. *J. Am. Chem. Soc.* **1993**, *115*, 6440-6441. (c) Hoffman, B. M.; Sturgeon, B. E.; Doan, P. E.; DeRose, V. J.; Liu, K. E.; Lippard, S. J. *J. Am. Chem. Soc.* **1994**, *116*, 6023-6024.
(14) (a) Fox, B. G.; Lipscomb, J. D. *Biochem. Biophys. Res. Commun.* **1988**, *154*, 165-170. (b) Fox, B. G.; Surerus, K. K.; Münck, E.; Lipscomb, J. D. *J. Biol. Chem.* **1988**, *263*, 10553-10556.
(15) Hendrich, M. P.; Fox, B. G.; Andersson, K. K.; Debrunner, P. G.; Lipscomb, J. D. *J. Biol. Chem.* **1992**, *267*, 261-269.
(16) (a) Pulver, S.; Froland, W. A.; Fox, B. G.; Lipscomb, J. D.; Solomon, E. I. *J. Am. Chem. Soc.* **1993**, *115*, 12409-12422. (b) Thomann, H.; Bernardo, M.; McCormick, J. M.; Pulver, S.; Andersson, K. K.; Lipscomb, J. D.; Solomon, E. I. *J. Am. Chem. Soc.* **1993**, *115*, 881-882.
(17) Hedman, B.; Co, M. S.; Armstrong, W. H.; Hodgson, K. O.; Lippard, S. J. *Inorg. Chem.* **1986**, *25*, 3708-3711.
(18) (a) Lippard, S. J. *Angew. Chem., Int. Ed. Engl.* **1988**, *27*, 344-361. (b) Sanders-Loehr, J. *Iron Carriers and Iron Proteins*; VCH Publishers Inc.: New York, 1989; pp 373-466. (c) Que, L., Jr.; True, A. E. *Prog. Inorg. Chem.* **1990**, *38*, 97-200.
(19) Rosenzweig, A. C.; Frederick, C. A.; Lippard, S. J.; Nordlund, P. *Nature* **1993**, *366*, 537-543.
(20) (a) Dalton, H. *Adv. Appl. Microbiol.* **1980**, *26*, 71-87. (b) Dalton, H. *Microbial Growth on C_1 Compounds*; Heyden Press: London, 1980; pp 1-10.
(21) Wu, W.; Rosenzweig, A. C.; Lippard, S. J. Unpublished results.

Table 1. Sample and Data Collection Summary[a]

sample	description	[Fe] (mM)	scans avg/scans collcd for EXAFS anal.[b]
Hsm	oxidized hydroxylase[c] noncomplexed	3.4	84/91, edge anal. only
HB-1	oxidized hydroxylase[c] w/component B	2.0	269/403
HB-3	oxidized hydroxylase[c] w/component B	1.5	398/442
HBr-1	oxidized hydroxylase[c] w/1-bromo-1-propene	3.2	226/234
HBr-3	oxidized hydroxylase[c] w/1-bromo-1-propene	1.8	230/260
HBr-4	oxidized hydroxylase[c] w/1-bromo-1-propene	1.9	124/143
HBBr-1	oxidized hydroxylase[c] w/component B and 1-bromo-1-propene	1.2	255/286
Hred[d]	reduced hydroxylase noncomplexed	4	91/91, edge anal. only
HB-2	reduced hydroxylase w/component B	0.9	448/481
HBr-2	reduced hydroxylase w/1-bromo-1-propene	1.7	276/286
HBBr-2	reduced hydroxylase w/component B and 1-bromo-1-propene	1.6	426/481

[a] All samples were run at SSRL on unfocused beamline 7−3 using Si(220) monochromator crystals. A 13-element solid state Ge fluorescence detector was used for the hydroxylase samples. [b] Each detector channel in the array detector is counted as giving one scan. [c] Sample was photoreduced to the semimet state by the X-ray beam. Only the scans after photoreduction was complete were averaged for further analysis. [d] The results of the EXAFS analysis for **Hred** have been previously reported;[12] however, edge data were collected for this study.

pene only or **HBBr** for samples with both component B and bromopropene), a 1000-fold excess of bromopropene (based on the concentration of protein, ~15 mg/mL) was added to ensure that the substrate would remain bound to the hydroxylase during the subsequent concentration procedure. The hydroxylase complexes were dialyzed first into a 5% ethylene glycol solution of 50 mM MOPS buffer (pH = 7.0) and then into a 50% ethylene glycol solution of the same buffer. For the **HBBr** samples and samples **HBr-2**, **HBr-3**, and **HBr-4**, the solutions contained a 10 000-fold excess of bromopropene. After dialysis, the samples were further concentrated on a Centricon centrifugal microconcentrator (Amicon), after which a 1000-fold excess of bromopropene was added to **HBr-2,3,4** and the **HBBr** samples. For **HBr-1**, no bromopropene was added until after the final concentration on the Centricon, at which point a 1000-fold excess was added.

The concentrated samples were degassed and brought into an anaerobic wetbox. The hydroxylase is isolated in its oxidized form; the reduced form was prepared by adding a 10-fold molar excess of sodium dithionite, 14 mM methyl viologen, and 4 mM proflavin to samples **HB-2**, **HBr-2**, and **HBBr-2** and incubating the samples for 40 min. The samples were then loaded into lucite EXAFS cells (23 mm × 2 mm × 3 mm; 140 μL) equipped with caps and with 25 μm Kapton windows, immediately frozen in liquid nitrogen upon removal from the box, and stored in a liquid nitrogen refrigerator.

EXAFS Data Collection. EXAFS and high-energy resolution edge scans were collected simultaneously by using a 1 mm vertical slit opening to maximize energy resolution and taking 0.15 eV steps over the edge region during an EXAFS scan. All of the samples were run on unfocused 8-pole wiggler beamline 7−3 (18 kG) at the Stanford Synchrotron Radiation Laboratory (SSRL), with the SPEAR ring operating at 3 GeV and 40−90 mA. A Si(220) double-crystal monochromator was used, detuned 45% at the end of the Fe EXAFS scan (7995 eV, k = 15 Å^{-1}) to minimize harmonic contamination in the incident beam. The data were measured in fluorescence mode at 10 K by using a continuous-flow LHe cryostat (Oxford Instruments, Model CF1208). The fluorescence signal was monitored with a 13-element Ge solid-state detector array[22] (Canberra) windowed on the Fe Kα signal (6840 eV). Total count rates of between 25 000 and 35 000 per second per channel (measured at 7995 eV detuned 45%) were maintained throughout the experiments. At these count rates, the detector was below saturation limits. One of the channels showed persistently high count rates; it was therefore not included in further data analysis.

Photoreduction of the Oxidized Hydroxylase Samples. As observed and discussed previously,[12,23] the oxidized samples of the hydroxylase are susceptible to photoreduction by the X-ray beam to the semimet state (Fe^{III}/Fe^{II}). Anticipating the photoreduction process, radiation from SSRL beamline 2−3 (unfocused bending magnet; Si(220) double crystal monochromator) was used to prephotoreduce **HB-3**, **HBBr-1**, and **HBr-3** (temperature 95−100 K, monochromator fully tuned at 7900 eV, slits 4 × 15 mm), as judged by monitoring the position of the edge as a function of time (~2.0 eV shift to lower energy occurs from oxidized to semimet form; the average time for photoreduction was ring current dependent, with a typical shift of ~1 eV/24 h on 2−3 and ~1 eV/2.5 h on 7−3 at 50 mA). After the prephotoreduction process, the samples were moved to beamline 7−3 for data collection and, in all cases, photoreduction of the samples continued for a few hours. Only the scans collected after the photoreduction process was judged to be complete were used for further data analysis. It should be noted that all originally oxidized samples discussed here were photoreduced to the semimet state by the X-ray beam, although only 3 samples were prephotoreduced on beamline 2−3.

EXAFS Data Reduction and Analysis. Data reduction and analysis were performed as described previously.[12,24] Information about the Fe concentration and scan averaging for the data sets is summarized in Table 1. Nonlinear least-squares curve-fitting techniques using empirical amplitude and phase parameters were used to analyze the k^3-weighted data, as described elsewhere.[25] The errors estimated in the EXAFS analysis with these protocols are ±0.02 Å in the distances and 25% in the coordination numbers.[25] The fits proceeded by allowing the initial coordination numbers and distances for an Fe−X pair of interest to vary.[26] Empirical amplitude and phase parameters were obtained as previously described.[12,23] Although earlier investigations[12,24] have revealed various difficulties arising from the application of experimentally derived amplitude and phase parameters in fits to second shell data, this fitting technique still provides the most reliable and accurate results for the first shells of the systems that we are investigating. A recent study has shown that the use of experimentally derived amplitude and phase functions obtained from EXAFS analysis of appropriate model compounds gives more accurate results in fits to metal foil EXAFS data than the use of theoretical amplitude and phase functions.[27]

Results

The k^3-weighted EXAFS of the photoreduced semimet complexed samples are presented along with the EXAFS data

(22) Cramer, S. P.; Tench, O.; Yocum, M.; George, G. N. *Nucl. Instrum. Methods Phys. Res.* **1988**, *A266*, 586−591.
(23) Ericson, A.; Hedman, B.; Hodgson, K. O.; Green, J.; Dalton, H.; Bentsen, J. G.; Beer, R. H.; Lippard, S. J. *J. Am. Chem. Soc.* **1988**, *110*, 2330−2332.
(24) DeWitt, J. G., Ph.D. Dissertation, Stanford University, 1993.
(25) (a) Cramer, S. P.; Hodgson, K. O.; Stiefel, E. I.; Newton, W. E. *J. Am. Chem. Soc.* **1978**, *100*, 2748−2761. (b) Cramer, S. P.; Hodgson, K. O. *Prog. Inorg. Chem.* **1979**, *15*, 1−39. (c) Scott, R. A. *Meth. Enzymol.* **1985**, *117*, 414−459.
(26) For all fits described in this paper, the EXAFS data from k = 3.5 to 12.5 Å^{-1} were Fourier transformed to R (Å) space to isolate the first and second shell contributions to the data. The individual contributions were isolated, backtransformed to k space, and fit from k = 4.0 to 12.0 Å^{-1}. In addition, both shells were backtransformed together and fit between k = 4.0 and 12.0 Å^{-1}, as were the unfiltered data. The windows used to isolate the peaks in the Fourier transforms for the backtransforms are presented in the tables of the fit results. A Gaussian window width of 0.1 Å was used to reduce truncation artifacts in the Fourier transforms.
(27) Koningsberger, D. C. *XAFS VII*; Kobe, Japan; Aug 1992, personal communication.

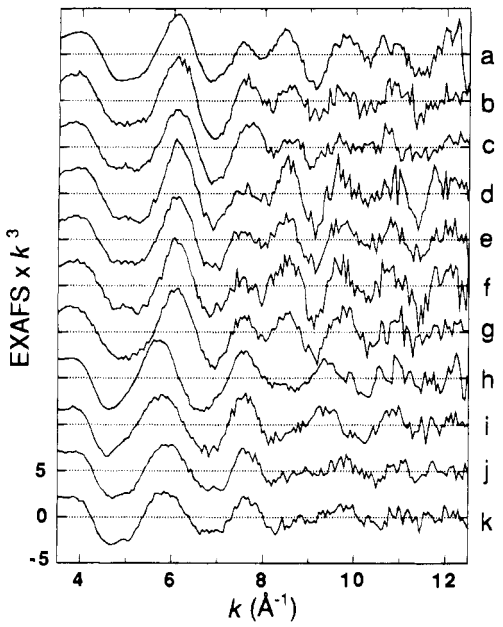

Figure 1. EXAFS of the semimet and reduced hydroxylase samples. Semimet hydroxylase samples: noncomplexed (a) **Hsm**; with component B (b) **HB-1**, (c) **HB-3**; with bromopropene (d) **HBr-1**, (e) **HBr-3**, (f) **HBr-4**; with B and bromopropene (g) **HBBr-1**. Reduced hydroxylase samples: noncomplexed (h) **Hred**; with bromopropene (i) **HBr-2**; with component B (j) **HB-2**; with B and bromopropene (k) **HBBr-2**. The data shown here are the data used for Fourier transforms (k = 3.5−12.5 Å^{-1}). Note the difference in the appearance of the EXAFS between k = 7 and 10 Å^{-1} for the semimet samples and above k = 8 Å^{-1} for the reduced samples.

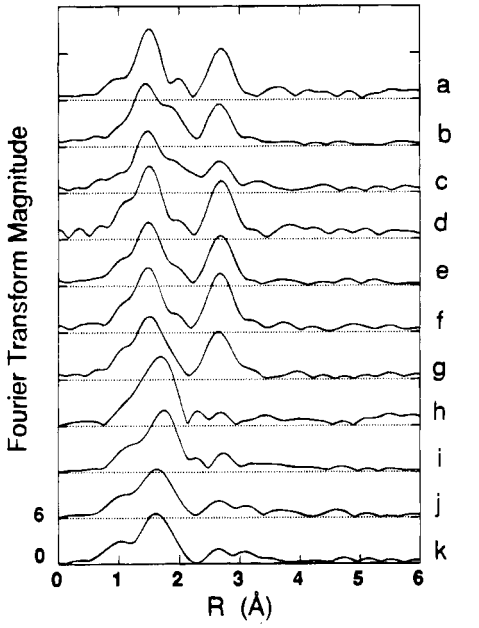

Figure 2. Fourier transforms (non-phase-corrected) of the semimet and reduced hydroxylase samples. Semimet hydroxylase samples: noncomplexed (a) **Hsm**; with component B (b) **HB-1**, (c) **HB-3**; with bromopropene (d) **HBr-1**, (e) **HBr-3**, (f) **HBr-4**; with B and bromopropene (g) **HBBr-1**. Reduced hydroxylase samples: noncomplexed (h) **Hred**; with bromopropene (i) **HBr-2**; with component B (j) **HB-2**; with B and bromopropene (k) **HBBr-2**.

of the noncomplexed semimet hydroxylase[12] (**Hsm**) in Figure 1a−g. The Fourier transforms (FT) of the data (over the k range 3.5−12.5 Å^{-1}) are presented in Figure 2a−g, along with FT data for the noncomplexed semimet hydroxylase. Visual inspection of the data reveals differences in the EXAFS of the complexed vs the noncomplexed forms of the hydroxylase. For noncomplexed hydroxylase (**Hsm**, Figure 1a), the maximum at k > 8 Å^{-1} is greater in amplitude than the maximum at k < 8 Å^{-1}; in the B-complexed samples (**HB-1**, Figure 1b, and **HB-3**, Figure 1c), the relative amplitudes of these maxima are reversed, and in the B plus bromopropene complex (**HBBr-1**, Figure 1g), the amplitudes are nearly equal. The minimum at k = 9 Å^{-1} is shallower for **HB-1** and **HB-3** than for **Hsm** or **HBBr-1**. The EXAFS of the hydroxylase in the presence of bromopropene (**HBr-1**, Figure 1d, **HBr-3**, Figure 1e, and **HBr-4**, Figure 1f) are very similar to the noncomplexed form (Figure 1a). It should be observed that the trends described are reproducible for measurements made on duplicate and triplicate independent samples (2 samples with component B, 3 samples with bromopropene).

The EXAFS data for the reduced samples are presented in Figure 1h−k, and the Fourier transforms of the data are given in Figure 2h−k. The data for the noncomplexed reduced hydroxylase (**Hred**)[12] are also included for comparison. The EXAFS of the hydroxylase in the presence of component B (**HB-2**, Figure 1j, and **HBBr-2**, Figure 1k) are shifted slightly to higher k, and the minimum at k ~8.5 Å^{-1} in the noncomplexed sample (**Hred**, Figure 1h) is not as distinct in the B−hydroxylase samples. The bromopropene−hydroxylase sample (**HBr-2**, Figure 1i) is more similar to the noncomplexed samples (Figure 1h); however, the ~8.5 Å^{-1} minimum is shifted somewhat to lower k for **HBr-2** relative to **Hred**. These differences in the EXAFS data are clearly seen in the Fourier transforms of the data (Figure 2h−k), with the R ~ 1.8 Å peak for the B-complexed forms of the hydroxylase (Figure 2j,k) appearing 0.08−0.09 Å to lower R than the peaks in the noncomplexed (Figure 2h) and bromopropene-complexed (Figure 2i) forms. Although the Fourier transforms above 2 Å are different for all of the reduced samples, there is no indication of a strong second shell Fe−Fe interaction, in striking contrast to that seen in the semimet samples (Figure 2a−g).

Results of Fits. *First Shell Fits.* Results of the fits for the Fourier-filtered first coordination sphere are presented in Table 2. The same trends in fits described previously[12] (two contributions required, two possible minima for fits with a N and an O contribution, no evidence for a μ-oxo feature) were seen for the analysis here. The detailed fit results are presented for **HB-1** to represent the trends seen in fits to all samples. For the other samples, the full results are provided as supplemental material in Table S-I. For **HB-2,3** and the **HBr** and **HBBr** samples, the fit results presented in Table 2 are consistent with the results of EPR studies suggesting a mixed N/O coordination[28] (and now known from the X-ray structure determination[19]) and with the fact that Fe−N bond distances are generally longer than Fe−O bond distances in dinuclear Fe compounds of this type. Due to the correlation of the N and O parameters for the limited k range of the data, we will initially describe the coordination-weighted average bond lengths[12] and later discuss trends in the individual Fe−N and Fe−O contributions.

The average first shell coordination spheres for all of the complexed forms of the semimet hydroxylase are very similar to one another. For semimet hydoxylase in the presence of component B, an average coordination of 6.4 N/O at 2.08 Å from Fe (fit HB-1E) was found for **HB-1** and of 5.7 N/O at 2.08 Å (fit HB-3A) for **HB-3**. The bromopropene-complexed form of the hydroxylase had an average Fe coordination of 5.6 N/O at 2.06 Å for **HBr-1** (fit HBr-1A) and 5.3 N/O at 2.07 Å

(28) The EPR signal at g_{av} < 2.0 and the value of the coupling constant (J = −32 cm^{-1} [12]) are consistent with a hydroxo/alkoxo/carboxylato bridged diiron center; ENDOR[13,15] and ESEEM studies suggest the presence of 2 N-donating groups coordinated to the Fe center.

Table 2. Results of First Shell Fits[a] to the Hydroxylase Data

sample	window width (Å)	fit	N		O		
			CN[b]	R (Å)	CN	R (Å)	F[c]
HB-1, semimet hydroxylase w/component B	0.70−2.35	HB-1A	2.1	2.07			1.2
		HB-1B			1.9	2.04	1.0
		HB-1C	4.1	2.15			0.28
			3.5	1.99			
		HB-1D			2.9	2.12	0.31
					2.5	1.96	
		HB-1E	3.5	2.17	2.9	1.98	0.29
		HB-1F	2.9	1.97	3.2	2.11	0.27
HB-3, semimet hydroxylase w/component B	0.75−2.40	HB-3A	3.0	2.17	2.7	1.98	0.39
HBr-1, semimet hydroxylase w/1-bromo-1-propene	0.75−2.30	HBr-1A	2.4	2.17	3.2	1.98	0.30
HBr-3, semimet hydroxylase w/1-bromo-1-propene	0.70−2.30	HBr-3A	2.5	2.18	2.8	1.98	0.25
HBr-4, semimet hydroxylase w/1-bromo-1-propene	0.70−2.25	HBr-4A	2.4	2.18	2.9	1.98	0.26
HBBr-1, semimet hydroxylase w/component B and 1-bromo-1-propene	0.70−2.20	HBBr-1A	2.5	2.17	2.8	1.99	0.30
HB-2, reduced hydroxylase w/component B	0.50−2.30	HB-2A	2.4	2.20	2.2	2.02	0.30
HBr-2, reduced hydroxylase w/1-bromo-1-propene	0.70−2.20	HBr-2A	3.0	2.20	1.8	2.04	0.31
HBBr-2, reduced hydroxylase w/component B and 1-bromo-1-propene	0.50−2.30	HBBr-2A	2.2	2.22	2.2	2.04	0.33

[a] Fitting range $k = 4-12$ Å^{-1}. Errors are estimated to be about ±0.02 Å for distances and 25% for coordination numbers.[25] [b] CN = coordination number. [c] $F = \{[k^6(\text{data}-\text{fit})^2]/(\text{no. of points})\}^{1/2}$.

Table 3. Results of Second Shell Fits[a] to the Hydroxylase Data

sample	window width (Å)	fit	Fe		C		
			CN[b]	R (Å)	CN	R (Å)	F[c]
HB-1, semimet hydroxylase w/component B	2.30−3.15	HB-1G	1.0	3.39			0.37
		HB-1H	0.6	3.01			0.65
		HB-1I			4.9	3.03	0.36
		HB-1J			3.7	3.38	0.74
		HB-1K	0.6	3.36	3.4	3.05	0.24
		HB-1L	1.3	3.42	3.4	3.39	0.31
		HB-1M	0.5	3.01	2.8	3.38	0.54
		HB-1N	0.3	2.93	5.1	3.04	0.27
HB-3, semimet hydroxylase w/component B	2.30−3.15	HB-3B	0.8	3.39			0.26
HBr-1, semimet hydroxylase w/1-bromo-1-propene	2.20−3.50	HBr-1B	1.5	3.41			0.62
HBr-3, semimet hydroxylase w/1-bromo-1-propene	2.20−3.45	HBr-3B	1.2	3.41			0.51
HBr-4, semimet hydroxylase w/1-bromo-1-propene	2.15−3.45	HBr-4B	1.4	3.41			0.75
HBBr-1, semimet hydroxylase w/component B and 1-bromo-1-propene	2.15−3.50	HBBr-1B	1.2	3.40			0.48

[a] Fitting range $k = 4-12$ Å^{-1}. Errors are estimated to be about ±0.02 Å for distances and 25% for coordination numbers.[25] [b] CN = coordination number. [c] $F = \{[k^6\ (\text{data}-\text{fit})^2]/(\text{no. of points})\}^{1/2}$.

for **HBr-3** and **HBr-4** (fits HBr-3A and HBr-4A, respectively). For hydroxylase in the presence of both component B and bromopropene (**HBBr-1**), the average first shell Fe coordination was found to be 5.3 N/O at 2.07 Å (fit HBBr-1A). No evidence of a short Fe−O contribution, which would indicate the presence of an oxo-bridged diiron center, was found. For the reduced forms of the hydroxylase, the average coordination number decreased and the average bond length increased relative to the semimet forms. For the reduced hydroxylase with component B (**HB-2**) a first shell coordination of 4.6 N/O at 2.11 Å (fit HB-2A) was found, consistent with the shift of the first peak in the Fourier transform to shorter R relative to the noncomplexed form (average first shell coordination ~5 N/O at 2.15 Å; ref 12). For reduced hydroxylase with bromopropene, the average Fe coordination of the first shell was 4.8 N/O at 2.14 Å (**HBr-2**, fit HBr-2A), and with both B and bromopropene (**HBBr-2**), the first shell was found to consist of 4.4 N/O at 2.13 Å (fit HBBr-2A).

Second Shell Fits. The results of second shell fits to the data are presented in Table 3. The detailed fit results are presented for **HB-1** to represent the trends seen in fits to all samples. For the other samples, the final results are summarized, but the full results are provided as supplemental material in Table S-II. We have previously described the bias of the second shell fits for the Fe−Fe distance corresponding to the distance in the model compound from which parameters were obtained.[12] However, on the basis of the absence of an oxo bridge in the Fe center, as determined from both EXAFS[12] and ENDOR,[13b,16b] a non-oxo-bridged model compound is the most appropriate for obtaining the empirical parameters.[12,29] For that reason, the hydroxo-bridged model $[Fe_2(OH)(OAc)_2(HB(pz)_3)_2](ClO_4)_2$ (3.4 Å Fe−Fe distance)[12,30] was used to extract parameters for analyzing the second shell Fe−Fe interaction.

For the semimet hydroxylase in the presence of component B (**HB-1** and **HB-3**), the best fit Fe-only minima corresponded to 1.0 and 0.8 Fe at 3.39 Å (fits HB-1G and HB-3B, respectively). The Fe−Fe coordination for the hydroxylase with bromopropene was found to be 1.5 Fe at 3.41 Å for **HBr-1** (fit HBr-1B), 1.2 Fe at 3.41 Å for **HBr-3** (fit HBr-3B) and 1.4 Fe at 3.41 Å for **HBr-4** (fit HBr-4B). For **HBBr-1**, the best Fe-only fit corresponded to 1.2 Fe at 3.40 Å (fit HBBr-1B). A second Fe-only minimum corresponding to a distance of ~3.0 Å (see for example fit HB-1H) was found for all samples. This second minimum is possibly due to coincidence of the Fe phase with the phase of the contribution from the low-Z atoms which

(29) Zhang, K.; Stern, E. A.; Ellis, F.; Sanders-Loehr, J.; Shiemke, A. K. *Biochemistry* **1988**, *27*, 7470−7479.
(30) Armstrong, W. H.; Lippard, S. J. *J. Am. Chem. Soc.* **1984**, *106*, 4632−4633.

Table 4. Results of Wide Shell Fits[a] to the Hydroxylase Data

sample	window width (Å)	fit	N		O		Fe		C		F[c]
			CN[b]	R (Å)	CN	R (Å)	CN	R (Å)	CN	R (Å)	
HB-1, semimet hydroxylase w/component B	0.70−3.15	HB-1O	3.5	2.16	2.8	1.97					0.96
		HB-1P	3.4	2.16	2.7	1.97	1.1	3.39			0.47
		HB-1Q	3.3	2.16	2.6	1.97	0.7	3.00			0.69
		HB-1R	3.4	2.16	2.7	1.97			3.6	3.38	0.82
		HB-1S	3.5	2.17	2.9	1.98			4.9	3.03	0.51
		HB-1T	3.4	2.17	2.8	1.98	0.7	3.37	2.6	3.05	0.42
HB-3, semimet hydroxylase w/component B	0.75−3.15	HB-3C	2.9	2.17	2.6	1.98	0.8	3.39			0.45
HBr-1, semimet hydroxylase w/1-bromo-1-propene	0.75−3.50	HBr-1C	2.5	2.17	3.1	1.97	1.5	3.41			0.68
HBr-3, semimet hydroxylase w/1-bromo-1-propene	0.70−3.45	HBr-3C	2.5	2.17	2.6	1.98	1.2	3.41			0.57
HBr-4, semimet hydroxylase w/1-bromo-1-propene	0.70−3.45	HBr-4C	2.5	2.17	2.8	1.97	1.4	3.41			0.79
HBBr-1, semimet hydroxylase w/component B and 1-bromo-1-propene	0.70−3.50	HBBr-1C	2.4	2.16	2.6	1.99	1.2	3.40			0.59

[a] Fitting range $k = 4-12$ Å^{-1}. Errors are estimated to be about ±0.02 Å for distances and 25% for coordination numbers.[25] [b] CN = coordination number. [c] $F = \{[k^6(\text{data-fit})^2]/(\text{no. of points})\}^{1/2}$.

Table 5. Results of Fits[a] to the Nonfiltered Hydroxylase EXAFS Data

sample	fit	N		O		Fe		C		F[c]
		CN[b]	R (Å)	CN	R (Å)	CN	R (Å)	CN	R (Å)	
HB-1, semimet hydroxylase w/component B	HB-1U	3.5	2.16	2.7	1.97					1.1
	HB-1V	3.5	2.16	2.7	1.97	1.1	3.39			0.72
	HB-1W	3.3	2.15	2.6	1.97	0.7	3.00			0.89
	HB-1X	3.4	2.16	2.7	1.97			4.0	3.37	0.98
	HB-1Y	3.5	2.17	2.9	1.98			4.9	3.02	0.78
	HB-1Z	3.4	2.16	2.8	1.97	0.8	3.37	2.2	3.06	0.70
HB-3, semimet hydroxylase w/component B	HB-3D	2.9	2.17	2.6	1.98	0.9	3.39			0.67
HBr-1, semimet hydroxylase w/1-bromo-1-propene	HBr-1D	2.4	2.16	3.0	1.97	1.5	3.41			1.0
HBr-3, semimet hydroxylase w/1-bromo-1-propene	HBr-3D	2.5	2.17	2.7	1.98	1.2	3.41			0.75
HBr-4, semimet hydroxylase w/1-bromo-1-propene	HBr-4D	2.6	2.17	2.8	1.97	1.4	3.41			1.1
HBBr-1, semimet hydroxylase w/component B and 1-bromo-1-propene	HBBr-1D	2.4	2.16	2.5	1.98	1.2	3.40			0.79
HB-2, reduced hydroxylase w/component B	HB-2B	2.3	2.11	2.1	2.03					0.68
	HB-2C	2.3	2.20	2.1	2.03	0.5	3.35			0.56
HBr-2, reduced hydroxylase w/1-bromo-1-propene	HBr-2B	3.1	2.19	1.7	2.04					0.69
HBBr-2, reduced hydroxylase w/component B and 1-bromo-1-propene	HBBr-2B	2.1	2.22	2.2	2.04					0.65

[a] Fitting range $k = 4-12$ Å^{-1}. Errors are estimated to be about ±0.02 Å for distances and 25% for coordination numbers.[25] [b] CN = coordination number. [c] $F = \{[k^6(\text{data-fit})^2]/(\text{no. of points})\}^{1/2}$.

are almost certainly present at ~3.0 Å from the Fe in bridged, dinuclear Fe centers.[17]

As described previously,[12] the second shell data can also be reasonably fit by using second shell Fe−C parameters without an Fe contribution at the same two distance minima obtained for the Fe-only fits to the data (see fits HB-1I and HB-1J). For fits including both Fe and C, there is a strong preference for the result consisting of a 3.4 Å Fe−Fe distance and a 3.0 Å Fe−C distance (compare fits HB-1K-N). These results suggest that there are two distance contributions to the second shell data at distances of 3.0 and 3.4 Å from the Fe center. The assignment of the longer distance as Fe and the shorter distance as C is consistent with the lack of an oxo-bridged diiron center, with the distribution of low-Z atoms in structurally characterized models,[29,30] and with the crystal structure results.[19]

In the combined Fe + C fits (Table S-II), an indication of a distance change in the second shell when component B is present was still apparent. In these fits, however, the Fe−C distance was decreased (as was the case for the C only fits), whereas the Fe−Fe distance was unchanged. Due to the high correlation between the two waves, it is not possible to establish whether the Fe−Fe, Fe−C, or both distances show a slight change. As discussed below, the empirical Fe−C amplitude and phase parameters are not reliable and were used mainly to illustrate the presence of a low-Z shell contribution. We therefore interpret the results as an Fe−Fe change but cannot exclude other possibilities.

Wide Shell Fits. The trends observed in the first and second shell fits to the semimet data were also seen in fits to the backtransform of both FT peaks. The final results are summarized in Table 4, and detailed fitting results are available in Table S-III. Only the results for $R_N > R_O$ are reported, although all of the fits with $R_N < R_O$ were performed. The fit function improved by a factor of 1.8−2 with the addition of a 3.4 Å Fe contribution to the N/O fit to the data (compare fits HB-1O and HB-1P) for all samples. The addition of both a 3.4 Å Fe and a 3.0 Å C contribution (fit HB-1T) only moderately improved the fit over the 3.4 Å Fe-only (fit HB-1P) or the 3.0 Å C-only fit (fit HB-1S).

Fits to the Nonfiltered Data. Fits to the nonfiltered data between $k = 4$ and 12 Å^{-1} were performed for all of the semimet and reduced samples (Table 5). Details of the fits are available in Table S-IV. All of the trends described above were seen for the fits to the nonfiltered data, although the fit functions were higher due to the increased noise level of the data. The data and the fits to the data (summarized in Table 5) for the semimet samples are shown in Figure 3.

For the reduced hydroxylase data, the N/O fits were adequate to explain the data; however, the broad feature on the low-k side of the 10 Å^{-1} maximum was not accounted for (Figure 4a,c,d). With the addition of ~2 C at 3.0 Å or ≤ 0.5 Fe at 3.4 Å, a better fit to the data at higher k was found (illustrated for **HB-2**, fit HB-2C, Table 5, Figure 4b). This result suggests that there is some high-frequency contribution to the data that can

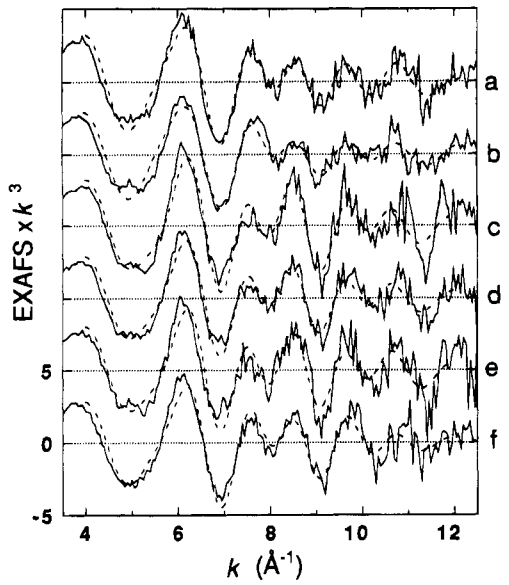

Figure 3. Fits to the nonfiltered data for the semimet hydroxylase samples (fitting range $k = 4-12$ Å^{-1}). The solid line is the data, and the dashed line is the fit to the data. The fit shown is the N, O, and Fe fit (Table 5). Key: (a) **HB-1**; (b) **HB-3**; (c) **HBr-1**; (d) **HBr-3**; (e) **HBr-4**; (f) **HBBr-1**.

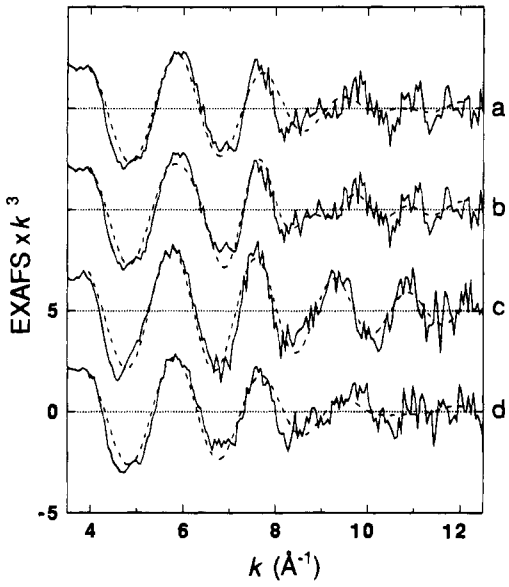

Figure 4. Fits to the nonfiltered data for the reduced hydroxylase samples (fitting range $k = 4-12$ Å^{-1}). The solid line is the data, and the dashed line is the fit to the data. The fit shown is the N and O fit (Table 5) with the exception of (b), which includes an Fe contribution. Key: (a) **HB-2**; (b) fit to **HB-2** with Fe, N, and O (Table 5, fit HB-2C); (c) **HBr-2**, (d) **HBBr-2**. Note that the inclusion of Fe to the fit for **HB-2** accounts for the shoulder in the EXAFS between $k = 8$ and 9 Å^{-1}.

be mathematically modeled with the Fe and C parameters but does not necessarily reflect the true second shell environment of the ferrous Fe center.

Contributions to the Differences Seen in the EXAFS Spectra. Although the average coordination environment for the Fe atoms does not change significantly due to the formation of complexes between the hydroxylase and component B and/or bromopropene, the individual contributions to the first and second shell fits do vary in a systematic and reproducible way, especially in the presence of component B. For both of the B-complexed samples **HB-1** and **HB-3**, the coordination number of the longer distance contribution is higher than the coordination number of the shorter distance contribution (Table 2, fit HB-1E and HB-3A). For noncomplexed semimet hydroxylase, the coordination number of the long distance contribution (2.5) is lower than the coordination number of the short distance contribution (3.1),[12] similar to the results seen for all three bromopropene-complexed samples (**HBr-1**, **HBr-3**, and **HBr-4**; Table 2, fits HBr-1A, HBr-3A, and HBr-4A). For the reduced samples, the coordination numbers are equal for the two contributions for the B-complexed samples (**HB-2**, **HBBr-2**; Table 2, fits HB-2A and HBBr-2A), but the coordination number for the long distance contribution (2.6) is lower than the short distance contribution (3.0) for the noncomplexed reduced sample.[12] For **HBr-2**, the coordination number for the long distance contribution is greater than the short distance contribution (Table 2, fit HBr-2A).

In the second shell data for the semimet samples plus component B only, the Fe–Fe distance is 3.39 Å for both samples measured, with an average coordination number of 0.9. For the three hydroxylase samples in the presence of bromopropene only, the Fe–Fe distance is consistently longer, at 3.41 Å, and the coordination number is higher as well (average 1.4). The difference in the coordination number for these two sets of samples is significant, greater than the 25% error estimated in this parameter determined by the EXAFS fits. Since a dinuclear Fe site is present in the samples, the noninteger coordination numbers reflect changes in the Debye–Waller factors of the Fe–Fe core, potentially accompanied by a rearrangement of the low-Z atoms in the second shell. While the exact nature of these differences in the individual N, O, and Fe contributions cannot be resolved by EXAFS over the range of data currently available, they are reflected in the systematic changes in the appearance of the EXAFS of the hydroxylase complexes compared to the noncomplexed hydroxylase samples.

Results of EXAFS Analysis with Brominated Substrate. To evaluate the detectability of Br on a ligand complexed to Fe, EXAFS data were collected on a brominated derivative of $Fe(acac)_3$, tris(3-bromo-2,4-pentanedionato)iron(III)[31] (or Fe-(3-Br-acac)$_3$). In this complex, the Fe$\cdots$Br distance is expected to be on the order of 5.2 Å.[32] The contributions of the three bromine atoms at this distance are clearly seen in the Fourier transform of Fe(3-Br-acac)$_3$ as compared to $Fe(acac)_3$ (Figure 5), suggesting that, at least in such a well-ordered structure, an Fe$\cdots$Br interaction at a distance as long as ~4–5 Å would be detectable by EXAFS. It should be pointed out that, although the amplitude of this Fourier transform feature is enhanced by multiple scattering since the Fe–C–Br angle is close to 180°, the backscattering amplitude and phase parameters for Br are very different from those of Fe and C, making Br more easily detected.

Inspection of the Fourier transforms of the semimet and reduced bromopropene complexes (**HBr-1**, **HBr-3**, **HBr-4**, **HBBr-1**, **HBr-2**, **HBBr-2**, Figure 2d–g,i,k) shows no suggestion of a strong interaction above 3.5 and 2.5 Å, respectively. If the Br were located in a well-ordered fashion around 3 Å

(31) Kluiber, R. W. *J. Am. Chem. Soc.* **1960**, *82*, 4839–4842.

(32) The crystal structure of the Fe complex has not been determined; the distance is based on the average Cr$\cdots$Br distance for a crystallographically characterized Cr dimer of the same ligand. Estes, E. D.; Scaringe, R. P.; Hatfield, W. E.; Hodgson, D. J. *Inorg. Chem.* **1977**, *16*, 1605–1610. The sample of Fe(3-Br-acac)$_3$ was diluted with BN powder, finely ground with a mortar and pestle, and pressed into a 1 mm Al spacer windowed with Mylar tape. The sample was run in transmission mode at SSRL on beamline 7–3 using a Si(220) monochromator detuned 50% at 7997 eV. The incident and transmitted beam intensity were monitored by using N_2-filled ionization chambers of standard design. The data were collected at 10 K, maintained by a continuous-flow LHe cryostat (Oxford Instruments Model CF1208).

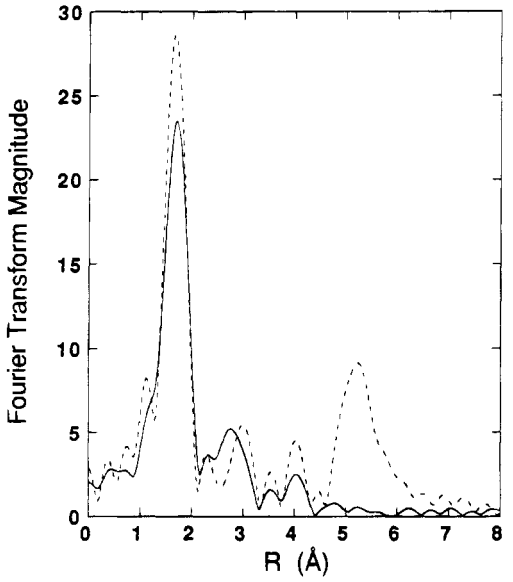

Figure 5. Fourier transforms of the EXAFS data for $Fe(acac)_3$ (solid) and $Fe(3\text{-}Br\text{-}acac)_3$ (dash). The peak at ~5 Å in the Fourier transform of $Fe(3\text{-}Br\text{-}acac)_3$ is due to the Fe···Br interaction.

from an Fe atom, it would be expected that the fit results to the second shell data would be significantly different for the hydroxylase samples with bromopropene from the non-bromopropene complexed samples. Such was not the case, however, and Br was not required to obtain excellent fits. The shorter limit of 2.5 Å for the reduced sample is especially clear, ironically, because of the absence of detectable Fe−Fe backscattering contribution around 3 Å (see Figure 2h−k).

X-ray Absorption Near-Edge Spectra. The Fe K-edge spectra of the hydroxylase samples are presented in Figure 6. The most intense transition seen in the X-ray absorption edge spectra (feature B) is due to the allowed 1s → 4p transition. To lower energy than this feature is the formally forbidden 1s → 3d transition (feature A) made allowed due to 4p orbital mixing into the 3d states as a result of symmetry distortions. For the semimet hydroxylase samples (Figure 6a), feature A appears at ~7114 eV, the main transition occurs at ~7129 eV (feature B), and there is a broad maximum at ~7134 eV (feature C). Relative to the pure hydroxylase, the intensity of feature B increases slightly in the presence of component B, and a prominent shoulder appears on the rising edge at ~7124 eV (feature A′). For the samples with only bromopropene added, there was irreproducibility in the presence/absence of any shoulder intensity depending on sample preparation (data not shown; although no difference was seen in the EXAFS data and results). There is no significant change in the intensity of feature A for all samples, and the energy position of the feature does not change.

The edges of the reduced hydroxylase complexes are compared in Figure 6b. Upon reduction to the diferrous state, the main transition moves as expected to lower energy (~7125 eV) and the shape changes dramatically, increasing in intensity and becoming more narrow compared to the semimet spectra. This change is typical of the reduction of Fe(III) to Fe(II) in models with mixed O and N ligation.[24] For the various reduced samples, the position of feature B does not change, but the intensity decreases in the spectra of the complexed samples relative to the noncomplexed sample. Among the hydroxylase complexes, the intensity of the feature is slightly greater for the hydroxylase sample in the presence of bromopropene than for the other samples. Additionally, a shoulder to the high energy side of feature B (feature C) at ~7131 eV appears for

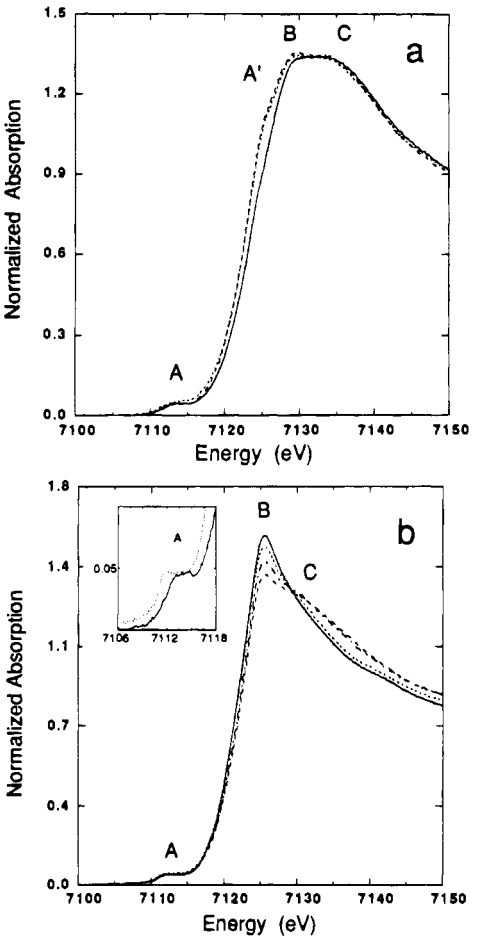

Figure 6. (a) Fe K-edge spectra of semimet hydroxylase samples: Noncomplexed sample, **Hsm** (solid); sample with component B, **HB-1** (dot); sample with B and bromopropene, **HBBr-1** (dash). Note the appearance of a shoulder on the rising edge in the spectra of the hydoxylase samples in the presence of B. (b) Fe K-edge spectra of reduced hydroxylase samples: Noncomplexed sample, **Hred** (solid); sample with bromopropene, **HBr-2** (dot); sample with B and bromopropene, **HBBr-2** (dash dot); sample with component B, **HB-2** (dash). Note that the intensity of the main feature decreases in the presence of component B and bromopropene. The inset shows the feature A for semimet **Hsm** (solid) and reduced **Hred** (dot) hydroxylase.

the hydroxylase in the presence of component B. Although the total intensity remains the same, the pre-edge feature (feature A) rises to a maximum more steeply for **Hred** and **HBr-2** than for **HB-2** and **HBBr-2** (data not shown), and the feature broadens relative to the pre-edge feature for the semimet samples (inset Figure 6b).

Discussion

Effect of Substrate and Component B on the Diiron Center. Perturbation in the EPR spectrum of the semimet hydroxylase in the presence of substrate was an early indication that the hydroxylase component interacted directly with substrate.[3c,20] In the presence of small molecules, the EPR spectrum was generally sharpened and intensified. The presence of component B, however, caused a dramatic difference in the EPR spectrum of the semimet hydroxylase from *M. trichosporium* OB3b.[8c] The hydroxylase no longer exhibited the g_{av} = 1.85 signal and a different saturation behavior was observed, resulting in an EPR signal with g_{av} = 1.75. These results suggest that the interaction of component B with the hydroxylase in its semimet form is more significant than the interaction of substrate. This interpretation is qualitatively supported by the EXAFS of the semimet and reduced samples (Figure 1). The

EXAFS of the samples with semimet hydroxylase and bromopropene (Figure 1d–f) is very similar to the noncomplexed EXAFS (Figure 1a), whereas the *EXAFS of the semimet hydroxylase with component B* (Figure 1b,c) *is different from that of the noncomplexed* form. The B plus bromopropene sample (Figure 1g) resembles a combination of the B–hydroxylase and the bromopropene–hydroxylase samples. The EXAFS of the reduced hydroxylase in the presence of component B (Figures 1j,k) is somewhat different from the noncomplexed form (Figure 1h) and the bromopropene complexed form (Figure 1i).

The presence of component B and substrate also alters the redox potentials of the hydroxylase Fe site.[10,11] The 15–20 mV decrease in redox potentials of the hydroxylase in the presence of substrate as compared to the redox potentials of the hydroxylase alone[10] suggests a slight decrease in the electron affinity of the Fe site in the presence of substrate. In the presence of stoichiometric amounts of component B and reductase, no reduction of the *M. capsulatus* hydroxylase occurred, suggesting that both component B and reductase are required to inhibit reduction of the hydroxylase. Earlier kinetic studies suggested that component B alone was responsible for the inhibition of the reduction of hydroxylase in the absence of substrate.[5,9] To produce the reduced hydroxylase XAS sample, the sample was treated with the reduction mediators in the presence of component B. The edge spectrum (Figure 6b) clearly indicates the reduced form of a diiron center; *therefore, reduction of the hydroxylase can proceed in the presence of component B and the absence of substrate*. This result supports the conclusion based on electrochemical studies[10a] that both the reductase and component B are required in the absence of substrate to inhibit effectively reduction of the *M. capsulatus* hydroxylase diiron site. More recent electrochemical experiments in the presence of component B alone further confirm that the hydroxylase can be reduced in this complex.[10b]

Effect of Complex Formation on the Hydroxylase. The average first shell coordination of the complexed forms of the semimet hydroxylase (5.3–6.4 N/O at 2.06–2.08 Å, Table 2) do not vary significantly from the average first shell coordination of the noncomplexed semimet hydroxylase (5.6 N/O at 2.08 Å).[12] On the basis of a comparison of the coordination-weighted average first shell data, the results suggest that no dramatic change in the coordination of the Fe occurs due to the formation of hydroxylase complexes with component B or substrate. There is, however, a systematic and reproducible difference in the individual N and O contributions to the first shell fits and in the Fe contribution to the second shell fits. These differences in the relative contributions are reflected by the differences seen in the EXAFS spectra of the various samples at $k \sim 8$ Å^{-1} discussed above. In particular, for the semimet samples the longer distance contribution to the Fe coordination environment increases in the presence of component B relative to the free hydroxylase and to the hydroxylase with bromopropene or both B and bromopropene present. Considering the Fe-only fits to the second shell data, the Fe coordination number is consistently lower for the B-complexed samples (**HB-1** and **HB-3**) than for the other samples, including the hydroxylase (CN = 1.1),[12] and the Fe–Fe distance is slightly shorter for the B only-complexed sample (3.39 Å, Table 3; the noncomplexed hydroxylase distance is 3.42 Å[12]). In the reduced samples, the two first shell contributions are about equal for the B-complexed samples (**HB-2** and **HBBr-2**), whereas for the other samples the distance distribution is uneven.

Given the inability of EXAFS to determine strictly the relative numbers of similar strength backscattering atoms, it is difficult to interpret the change in the contributions of the individual waves. The reproducibility of the results among independent samples of the same complex (2 samples with component B, 3 with bromopropene) does indicate, however, that a change occurs in the coordination of the diiron center as a result of complex formation with component B. Whether the origin of the difference arises from a change in the ligation of the Fe atoms, a distortion of the coordination environment, or a change in the covalency of the metal site can not be determined on the basis of EXAFS analysis of the available data.

Inspection of the crystal structure of the hydroxylase component[19] shows that the dinuclear Fe center lies in a 4 helix bundle. Two of the surrounding helices form one wall of a canyon which lies between the 2 $\alpha\beta\gamma$ subunits that comprise the hydroxylase dimer. This canyon has been suggested to be the docking site of component B, where interactions with the helices forming the wall of the canyon could modulate the Fe coordination in the active site. In particular, such interactions could affect two glutamate residues, Glu 209 and Glu 243, which coordinate the same Fe atom. Interaction of component B with the hydroxylase in this manner would be consistent with the results of magnetic circular dichroism (MCD) studies of the reduced hydroxylase with component B,[16a] which indicate that the environment of only one of the Fe atoms is altered in the component B complex. A shift in the coordinating mode of one or more of the glutamate residues (carboxylate shift[33]) could explain the subtle change in the distribution of distances seen in the EXAFS results described above, as well as the perturbation in the redox potentials[10,11] and the EPR signal[8c] seen for the hydroxylase/component B complex.

Location of the Substrate Binding Site. Although it is known that substrate interacts with the hydroxylase component, the location of the binding site has not been determined. In the crystal structure, there is a large hydrophobic pocket adjacent to the pocket containing the dinuclear Fe center, as well as a number of hydrophobic pockets between the active site and the second domain of the protein structure.[19] These hydrophobic pockets may provide access to the active site for substrate *via* conformational changes possibly triggered by interactions between the hydroxylase and component B or the reductase component of the MMO system. Moreover, it is known from ENDOR studies of the DMSO adduct of the mixed-valent hydroxylase from *M. capsulatus* that the oxygen atom of this inhibitor coordinates directly to the ferric center.[34] It is therefore conceivable that an olefin might similarly coordinate to such a site during the catalytic mechanism. If 1-bromo-1-propene were to form a π complex with one of the Fe atoms, the nonbonded Fe···Br distance would be ~3.25 Å, as determined by simple geometric considerations based on structurally characterized inorganic complexes. This brominated substrate was used for the hydroxylase/substrate complex to seek information about the proximity of the substrate binding site to the Fe center. Bromine is a stronger backscatterer than Fe, so an Fe···Br interaction should be detected if the substrate were to bind close enough to an Fe atom in an ordered configuration (with little rotational or vibrational motion). Under such circumstances, EXAFS should be sensitive to a Br interaction within ~4.0 Å. It might therefore be possible to determine the distance to the substrate binding site.

Inspection of the Fourier transforms of the reduced hydroxylase with bromopropene (Figure 2i,k) shows no indication of a

(33) Rardin, R. L.; Tolman, W. B.; Lippard, S. J. *New J. Chem.* **1991**, *15*, 417–430.
(34) DeRose V. J.; Liu, K. E.; Lippard, S. J.; Hoffman, B. M. Submitted for publication.

strong backscattering atom above 3 Å. Assuming that bromopropene is indeed bound in the hydrophobic pocket at the active site, these results conclusively demonstrate that the olefin does not form a π complex (η^2-coordination) with one of the Fe atoms. Since rotational disorder about the Fe−centroid in such a π complex would not alter the Fe···Br distance, this conclusion is valid even with the caveats about the disorder discussed below. For the semimet samples, no increase in intensity of the second shell peak, nor any indication of an additional outer shell backscattering atom, is seen in the Fourier transforms (Figure 2d−g). Given that the semimet second shell data can be well explained by only Fe and C contributions, and the absence of a longer distance peak in the reduced samples, these results suggest that substrate does not bind directly to the Fe atoms in an ordered fashion. The possibility that the Br is located near to the Fe atoms in a disordered configuration cannot be eliminated, however. Independent evidence for ligand binding at a location other than the Fe center of the reduced hydroxylase is provided by circular dichroism (CD) studies in the presence of a variety of anionic ligands, substrates, and inhibitors.[16a] In these studies, no change was seen in the CD spectra of the hydroxylase, suggesting that these molecules do not bind directly to the Fe atoms.

Multiple Scattering Effects. Multiple scattering interactions from the presence of rigid ligand groups such as imidazoles can often contribute significantly to the outer shell data.[35,36] It is likely that there are multiple scattering contributions to the second shell hydroxylase data which are not adequately modeled by the single-scattering fitting approach used here and which complicate the interpretation of the EXAFS of the outer shells. The possibility that multiple scattering from other ligand groups bound to the Fe atom is contributing to the second shell data cannot be eliminated. A very recent multiple scattering analysis of $Fe(acac)_3$[37] has revealed that there is a very strong contribution to the second shell data from a multiple scattering pathway involving the Fe−O−C unit (Fe−O−C angle 129°). This second shell has frequently been used, including in the present study, to extract second shell Fe−C amplitude and phase parameters. Since one can only assume transferability in the second shell if the two distances and the angle are the same, the parameters from $Fe(acac)_3$ are ill-suited to fit an averaged second Fe−C shell with many contributions.

This kind of Fe−O−C geometry may be similar to ligation of metal sites in proteins by carboxylate groups; indeed, the crystal structure of ribonucleotide reductase R2[38] shows an aspartate group coordinated to a single Fe atom in a similar bidentate mode. The glutamate residues in the MMO hydroxylase active site coordinate the Fe atoms in a monodentate mode with the exception of the bidentate bridging glutamate.[19] It is possible that multiple scattering will contribute for the monodentate geometrical configuration of carboxylate ligands in dinuclear metal centers as well. An understanding of the multiple scattering contributions and the development of a protocol which properly accounts for both the multiple and single scattering interactions will be an important step in the reliable application of the EXAFS technique to second shell data in dinuclear metalloprotein systems. With the emergence of the theoretical fitting codes FEFF[39] and GNXAS,[37,40] a systematic investigation of theoretical fitting approaches to dinuclear Fe centers is being conducted for eventual comparison to the results obtained from the use of empirically derived amplitude and phase parameters presented herein.

Interpretation of the Hydroxylase Edge Spectra. The weak pre-edge feature seen well below the 4p transition in transition metal spectra has been assigned to a formally dipole-forbidden 1s → 3d transition made allowed by 4p mixing into the 3d states as a result of symmetry distortions and vibronic coupling.[41,42] The intensity of this feature is inversely proportional to the symmetry of the metal site and increases as the metal site is distorted from octahedral to tetrahedral symmetry. The intensity of the feature can therefore be used to infer the coordination number and/or site symmetry of the metal atom.[43] The presence of the 1s → 3d feature in the edge spectra of the hydroxylase samples (Figure 6, feature A) indicates that the Fe site is distorted from octahedral symmetry. The intensity of this transition is consistent with the known 5−6 atom coordination of the Fe site in the MMO hydroxylase.[19] Within the noise level of the current data no significant intensity change is observed, indicating that there is no drastic change in symmetry upon complexation.

The appearance of the shoulder on the rising edge of the semimet hydroxylase spectra (feature A′, Figure 6a) is similar to changes seen in the edge spectra of Cu and Fe systems as a result of an increase in the covalency of the metal site.[41,44] In the Cu systems, this feature has been assigned as a ligand-to-metal charge transfer (LMCT) shake-down feature[45] associated with the 1s → 4p transition. If feature A′ reflects covalency in the Fe site, then the improved resolution of this feature in the hydroxylase complexes suggests that the covalency of the Fe site may increase as a result of the interaction with component B and possibly with bromopropene. The change in the redox potentials of the hydroxylase in the presence of propylene is consistent with a decrease in the electron affinity (and hence an increase in the covalency) of the Fe(III) center[10,11] suggesting

(35) Co, M. S.; Scott, R. A.; Hodgson, K. O. *J. Am. Chem. Soc.* **1981**, *103*, 986−988.
(36) Hasnain, S. S., Ed. *Synchrotron Radiation and Biophysics*; Ellis Horwood Ltd.: Chichester, U.K., 1990; Chapters 3 and 4.
(37) Westre, T. E.; Di Cicco, A.; Filipponi, A.; Natoli, C. R.; Hedman, B.; Solomon, E. I.; Hodgson, K. O. *J. Am. Chem. Soc.* **1995**, *117*, 1566−1583.
(38) Nordlund, P.; Sjöberg, B.-M.; Eklund, H. *Nature* **1990**, *345*, 593−598.
(39) Mustre de Leon, J.; Rehr, J. J.; Zabinsky, S. I.; Albers, R. C. *Phys. Rev. B* **1991**, *44*, 4146−4156.
(40) Filipponi, A.; Di Cicco, A.; Tyson, T. A.; Natoli, C. R. *Solid State Commun.* **1991**, *78*, 265−268.
(41) Shulman, R. G.; Yafet, Y.; Eisenberger, P.; Blumberg, W. E. *Proc. Natl. Acad. Sci. U.S.A.* **1976**, *73*, 1384−1388.
(42) This feature could also be caused by a quadrupole transition, in which case the selection rule is +2 and the 1s → 3d transition is allowed. The authors of ref 41 estimated that the quadrupole transition intensities would in general be 3 orders of magnitude weaker than the intensity of the Fe pre-edge feature and concluded that the feature is due to an Fe 1s → 3d transition made allowed by vibronic coupling of the 4p and 3d states. Experimental evidence clearly indicates, however, the presence of a quadrupolar component to the intensity of the 1s → 3d in $CuCl_4^{2-}$ (see: Hahn, J. E.; Scott, R. A.; Hodgson, K. O.; Doniach, S.; Desjardins, S. R.; Solomon, E. I. *Chem. Phys. Lett.* **1982**, *88*, 595−598) and it is expected based upon theoretical and experimental considerations to contribute to the intensity of this transition for Fe as well. The details of these effects for Fe edges are the subject of a experimental and theoretical study which will soon be submitted for publication (Westre, T. E.; Hedman, B.; Hodgson, K. O.; Solomon, E. I.).
(43) Roe, A. L.; Schneider, D. J.; Mayer, R. J.; Pyrz, J. W.; Que, L., Jr. *J. Am. Chem. Soc.* **1984**, *106*, 1676−1681.
(44) Kau, L.-S.; Spira-Solomon, D. J.; Penner-Hahn, J. E.; Hodgson, K. O.; Solomon, E. I. *J. Am. Chem. Soc.* **1987**, *109*, 6433−6442.
(45) The LMCT shake-down transition involves the transfer of an electron from the valence level of the ligand to the metal 3d manifold made possible by final state relaxation. This transition occurs at an energy below that of the metal 1s → 4p transition by an amount equal to the energy difference between the ligand valence and metal 3d orbitals. The position of the LMCT shake-down feature would be expected to move to lower energy as the covalency of the ligands increases because the valence energy level of a more covalent ligand would be higher than that of a less covalent ligand resulting in a larger energy difference between the ligand and metal orbitals.

that there is a correlation between complex formation and Fe center covalency in the hydroxylase.

In the edge spectra of the reduced hydroxylase samples (Figure 6b), the intensity of the 1s → 4p transition decreases in the order of noncomplexed hydroxylase (**Hred**), hydroxylase with bromopropene (**HBr-2**), hydroxylase with both B and bromopropene (**HBBr-2**), and hydroxylase with B (**HB-2**). The reduction in the intensity of the 1s → 4p transition is consistent with a change in the coordination of the Fe active site for ferrous compounds,[46] both with a reduction in the coordination number of the Fe atoms or with a distortion in the symmetry of the Fe coordination. This interpretation is in turn consistent with the change in the distance distribution seen in the EXAFS results, as well as with EPR[8c] and MCD[16a] studies of the hydroxylase/component B complex which suggest that the interaction with component B has an effect on the coordination environment of the diiron center. The presence of component B also gives rise to a high-energy shoulder (feature C) in the spectra of the reduced hydroxylase samples.

The pre-edge feature is quite wide for the reduced samples, suggesting that more than one transition is occurring. The 1s → 3d feature appears to be split by about 2 eV in the complex formed with bromopropene (**HBr-2**) and in the noncomplexed form (**Hred**). Splitting seen in ferrous compounds has been attributed to transitions to the ^{4}F (lower energy transition) and ^{4}P (higher energy transition) multiplet levels of the d^7 final state,[41] with a relative intensity of 7:3 for the ^{4}F:^{4}P splitting. Due to the noise level and the reduction in intensity of the leading edge of the feature for the B-complexed forms, it cannot be firmly established if the intensities of the features in the pre-edge region corresponds to the predicted intensity ratio for the ^{4}F to ^{4}P split.

Conclusions

The results of the EXAFS analysis for the range of data available do not show any dramatic change in the *average* coordination environment of the Fe center but suggest that a subtle change in the Fe center occurs due to complex formation. The presence of component B *does* have an effect on the first shell of the hydroxylase active site, reflected in the change in the distance distribution of the individual contributions to the first shell data (Table 2). Furthermore there is a minor decrease in the Fe−Fe distance and an increase in the Debye−Waller factor for the Fe−Fe interaction. Possible explanations for the difference seen in the distance distribution include distortion of the Fe environment, changes in the ligation of the Fe atoms, and/or a change in the covalency of the Fe site due to an interaction between component B and the Fe-coordinating helices in the hydroxylase. It must be noted, however, that if component B were to bind to the Fe center such that no net change occurred in the Fe coordination (for example if a carboxylate group were displaced by another carboxylate group), the EXAFS technique would not be sensitive to such an exchange. Other techniques have determined that component B has an effect on the diiron center[8c,16a] and a docking site for component B has been proposed from the crystal structure[19] which would perturb helices coordinating the Fe atoms in the hydroxylase. On the basis of a comparison of the Fourier transforms of the bromopropene−hydroxylase samples and Fe(3-Br-acac)$_3$, the Fe···Br distance is >3.5 Å. This result proves that if bromopropene is indeed in the hydrophobic pocket at the catalytic center, it does not coordinate in an η^2 mode to an Fe atom. Such a conclusion applies even if the substrate is bound in a rotationally disordered configuration. The appearance of a shoulder on the rising edge of the spectra of the semimet samples suggests that the covalency of the diiron center changes due to the presence of component B. The reduction in edge intensity of the reduced hydroxylase/component B complex relative to the noncomplexed hydroxylase is consistent with a change in the coordination environment in the diiron centers. These studies suggest that the changes which occur in the hydroxylase diiron center in the presence of the component B or substrate involve subtle perturbations in the coordination environment of the Fe atoms accompanied by changes in the electronic structure of the Fe center. Taken together, all of the techniques used to investigate the interaction between component B, substrate, and the hydroxylase, including XAS, are consistent only with indirect effects on the diiron center in the hydroxylase.

Acknowledgment. The data were collected at the Stanford Synchrotron Radiation Laboratory, which is supported by the Department of Energy, Office of Basic Energy Sciences, Divisions of Chemical Sciences and Materials Sciences, and the Department of Energy, Office of Health and Environmental Research. SSRL is also supported by the National Institutes of Health, Biomedical Research Technology Program, National Center for Research Resources (Grant RR-01209). Grant support was provided by the National Science Foundation (CHE-9121576 to K.O.H.) and the National Institute of General Medical Sciences (GM-32144 to S.J.L.).

Supplementary Material Available: Tables of EXAFS data (13 pages). Ordering information is given on any current masthead page.

(46) Westre, T. E. Personal communication.

IC9409930